Scientia Pharmaceutica

Article

In Vitro Inhibitory Activities against α-Glucosidase, α-Amylase, and Pancreatic Lipase of Medicinal Plants Commonly Used in Chocó (Colombia) for Type 2 Diabetes and Obesity Treatment

Kevin P. Lévuok-Mena [1], Oscar J. Patiño-Ladino [2] and Juliet A. Prieto-Rodríguez [1,*]

[1] Departamento de Química, Facultad de Ciencias, Pontificia Universidad Javeriana, Bogotá 110231, Colombia; rivask@javeriana.edu.co
[2] Departamento de Química, Facultad de Ciencias, Universidad Nacional de Colombia, Sede Bogotá, Bogotá 111321, Colombia; ojpatinol@unal.edu.co
* Correspondence: juliet.prieto@javeriana.edu.co; Tel.: +57-6013208320 (ext. 4124)

Abstract: Plant-based therapies are widely utilized for treating diseases in approximately 80% of the global population, including Colombia's Chocó Department. This study aimed to identify and evaluate plants with significant therapeutic value for obesity and diabetes in Chocó. The inhibitory effects of these plants on pancreatic lipase (PL), α-glucosidase (AG), and α-amylase (AA) were assessed, and the most promising species were selected to isolate and identify bioactive components. *Artocarpus altilis*, *Momordica balsamina*, *Bauhinia picta*, *Neurolaena lobata*, and *Vismia macrophylla* emerged as key species based on their traditional usage among the Chocó population. Notably, the extract derived from *Vismia macrophylla* demonstrated the most encouraging outcomes as a digestive enzyme inhibitor, exhibiting IC_{50} values of 0.99 ± 0.21 μg/mL, 5.61 ± 0.82 mg/mL, and 28.91 ± 2.10 μg/mL for AG, AA, and PL, respectively. Further chemical analysis led to the isolation of three bioactive compounds: 5′-demethoxycadensin G **1**, para-hydroxybenzoic acid methyl ester **2**, and para-hydroxybenzoic acid butyl ester **3**. Compound **1** displayed the highest activity against AG (IC_{50} = 164.30 ± 0.11 μM), while compounds **2** (IC_{50} = 28.50 ± 4.07 μM) and **3** (IC_{50} = 10.15 ± 3.42 μM) exhibited potent inhibitory effects on PL. Molecular docking and enzymatic kinetics studies indicate that these bioactive compounds primarily act as mixed inhibitors of AG and non-competitive inhibitors of PL. These findings underscore the potential of V. macrophylla and its compounds as effective inhibitors of digestive enzymes associated with obesity and type 2 diabetes.

Keywords: vismia macrophylla; artocarpus altilis; momordica balsamina; bauhinia picta; neurolaena lobata; α-glucosidase; α-amylase; pancreatic lipase

check for updates

Citation: Lévuok-Mena, K.P.; Patiño-Ladino, O.J.; Prieto-Rodríguez, J.A. In Vitro Inhibitory Activities against α-Glucosidase, α-Amylase, and Pancreatic Lipase of Medicinal Plants Commonly Used in Chocó (Colombia) for Type 2 Diabetes and Obesity Treatment. *Sci. Pharm.* **2023**, *91*, 49. https://doi.org/10.3390/scipharm91040049

Academic Editors: Marta Menegazzi and Murali Mohan Yallapu

Received: 29 April 2023
Revised: 27 July 2023
Accepted: 12 September 2023
Published: 18 October 2023

1. Introduction

Obesity is a multifactorial and inflammatory metabolic disease characterized by endocrine dysfunction [1]. This chronic condition is considered a major risk factor for the development of non-communicable diseases such as type 2 diabetes, hypertension, dyslipidemia, cardiovascular disease, and some cancers [2,3]. The World Obesity Foundation estimates that by 2030, approximately one billion people worldwide will be living with obesity [4]. The increase in the prevalence, incidence, and morbidity of obesity is directly related to the global rise in diabetes [5]. In 2017, approximately 462 million people were affected by type 2 diabetes, accounting for 6.28% of the world's population (4.4% of those aged 15–49, 15% of those aged 50–69, and 22% of those aged 70 and older). Diabetes alone causes over 1 million deaths annually, making it the ninth leading cause of death [6]. According to the International Diabetes Federation (IDF), it is projected that approximately 537 million people worldwide will be living with diabetes in 2021, and the global prevalence of type 2 diabetes is expected to increase to 783 million by 2045 [7]. These projections highlight the need for new therapeutic strategies to treat and control diabetes and obesity.

There are three approaches to treating being overweight, obesity, and diabetes: lifestyle modification, pharmacotherapy, and bariatric surgery. The most effective approach combines behavioral strategies, diet, and exercise with pharmacotherapy aimed at delaying the absorption of dietary fats and carbohydrates [8]. α-Glucosidase (AG) is an exo-type carbohydrate-splitting enzyme secreted by the intestinal epithelium (enterocytes, brush border cells) [9]. Inhibiting this enzyme is one of the best strategies to lower glucose levels in the blood plasma, as it delays carbohydrate digestion, thereby helping to prevent the occurrence of late diabetic complications. It has become one of the therapeutic approaches for newly diagnosed diabetics [10–12]. α-Amylase (AA) is a calcium metalloenzyme that hydrolyzes starch, breaking down α-1,4 glycosidic bonds in amylose to yield maltose and glucose [13]. Inhibiting this enzyme slows carbohydrate digestion and glucose absorption, helping to reduce hyperglycemia, obesity, and problems such as being overweight [14]. Pancreatic lipase (PL) is the key enzyme in fat digestion, responsible for hydrolyzing 50–70% of total dietary fats, breaking down triacylglycerols into free fatty acids and monoacylglycerols in the intestinal lumen [15]. Inhibitors of PL have gained attention as a potential approach to treating obesity by reducing fat absorption [16–18]. Various drugs that inhibit digestive enzymes, such as orlistat, acarbose, voglibose, and miglitol, are widely used to treat diabetes and obesity. However, these drugs have been reported to be expensive, with low therapeutic efficacy and associated side effects [8,13]. Consequently, several studies highlight the importance of exploring new therapeutic alternatives for the treatment of diabetes and obesity, particularly focusing on the inhibition of digestive enzymes [19].

Recent research has focused on traditional herbal medicines and their active phytoconstituents used worldwide to lower blood glucose levels and body weight [20]. Over the past decades, extensive screening of natural products has demonstrated their potential as sources for drug discovery. However, only a few plant-based drugs have been scientifically validated [21]. The classical approach to natural-product-based drug discovery involves screening "crude" extracts to identify bioactive compounds, which are then further isolated from the extracts [22]. Through ethnopharmacological and phytochemical approaches, certain South American plants used for medicinal purposes have been identified as promising sources of bioactive inhibitors of AG, AA, and PL [15,23–27]. In the Colombian Pacific region, the prevalence of obesity and diabetes among Afro-indigenous peoples is strongly influenced by socioeconomic and cultural context, as well as genetic ancestry [28]. However, many of these individuals do not have access to the public health system. Consequently, various traditional herbal remedies are widely produced and consumed in this region, providing an affordable and effective therapeutic means to combat the increase in obesity, diabetes, and the high cost of modern medicine. The commercial network of traditional healers, specialized plant markets, and practitioners of this ethnotherapeutic system represents a prominent manifestation of this ancient practice. Although there are compilations of plants used to treat obesity and diabetes in the Colombian Pacific, there is a lack of ethnopharmacological and scientific studies confirming their traditional uses, especially for the inhibition of digestive enzymes. Therefore, conducting such studies is crucial to preserve and document the traditional knowledge of promising plants with therapeutic potential, as a strategy for the conservation, and rational and sustainable use of Colombian Pacific biodiversity, particularly in the Chocó region. The objective of this study was to experimentally demonstrate the inhibitory effects of AG, AA, and PL obtained from various plants used in traditional medicine in the Colombian Pacific against obesity and diabetes, as well as to identify some bioactive components of the most promising species.

2. Materials and Methods

2.1. General Experimental Procedures

All commercially available reagents were used without further preparation, while solvents were of technical grade and distilled before use. Thin-layer chromatography (TLC) was performed on SiliaPlateTM alumina plates coated with silica gel 60 F254 (SiliCycle® Inc., Quebec City, QC, Canada). Vacuum liquid chromatography (VLC) was performed

on SiliaPlateTM silica gel F254 of size 5–20 µm (SiliCycle® Inc., QC, Canada). Flash chromatography (FC) was performed on SiliaFlash® silica gel P60 of size 40–63 µm (SiliCycle® Inc., Quebec, QC, Canada). Melting points were recorded using a Thermo Scientific 00590Q Fisher-John's instrument (Thermo Scientific®, Waltham, MA, USA). NMR measurements were performed using a Bruker Advance AC-300 spectrometer (Bruker®, Hamburg, Germany) for ^{1}H NMR and APT experiments at 300 MHz for 1H and 75 MHz for APT. In addition, ^{1}H-^{1}H, direct ^{1}H-^{13}C, and long-range ^{1}H-^{13}C scalar spin–spin connectivity was determined by 2D spectroscopic analysis of COSY, HMQC, and HMBC experiments. Chemical shifts (δ) were expressed in parts per million (ppm) and coupling constants (J) in Hz. The following abbreviations were used to denote chemical shift multiplications: s = singlet, d = doublet, t = triplet, q = quartet, m = multiplet, bs = broad singlet.

The enzymes used for the enzyme inhibition studies were pancreatic lipase type 2 (PL) from porcine pancreas (100–400 units/mg protein, L-SLBD2433V, Sigma-Aldrich, Saint Louis, MI, USA; EC. 3.1.1.3); α-amylase (AA) type VI-B from porcine pancreas (≥10 units/mg solid, L-SLBP4061V, Sigma-Aldrich; EC. 3.2.1.1); and α-glucosidase (AG) type I from *Saccharomyces cerevisiae* (lyophilized powder, ≥10 units/mg protein, L-SLBX6245, Sigma-Aldrich; EC 3.2.1.20). The following compounds were used as substrates: 4-nitrophenyl butyrate (Sigma-Aldrich) for PL, soluble potato starch (Sigma-Aldrich), and 3,5-dinitro salicylic acid (DNA, as derivatization reagent) were used for AA and 4-nitrophenyl-α-D-glucopyranoside (Sigma-Aldrich) for AG. Absorbance measurements were performed with a Thermo Scientific Multiskan GO microplate reader (Waltham, MA, USA) using Skanlt RE4.1 software.

2.2. Study Area

Quibdó is a province located in the central part of Chocó, in northwestern Colombia. It is situated at a latitude of 5°42′00″ N and a longitude of 76°40′00″ W. The province covers an area of 3337.5 km^2 and has a population of 97,714 inhabitants (source: https://www.quibdo-choco.gov.co/Paginas/default.aspx, accessed on 15 March 2023) (Figure 1). Most of the area is covered by tropical rainforests, accounting for 98% of the land. Quibdó is composed of 29 districts, including Altagracia, Alto Munguidó, Barranco, Bella Luz, Boca de Naurita, Boca de Nemotá, Boca de Tanando, Calahorra, Campo Bonito, El Fuerte, El Tambo, Guadalupe, Guarandó, Guayabal, Gitradó, La Troje, Las Mercedes, Mojaudó, Pacurita, Puerto Murillo, Sanceno, De la Rosa, San Francisco de Icho, San Rafael de Negua, Tagachi, Tutunendo, Villa del Rosario, and Winandó.

2.3. Ethnopharmacological Study and Determination of Use Value (UV) of Medicinal Plants

This study was conducted following the method proposed by Cruz and Andrade-Cetto [29]. Interviews were carried out using questionnaires with semi-structured questions, consisting of three parts: (A) general information, (B) ethnomedical information, and (C) ethnobotanical uses. Verbal information was obtained from each participant after informing them about the purpose of our research and obtaining their voluntary informed consent to participate in the study. Thus, twenty medicinal plant sellers (nineteen women, one man), twenty diabetes/obese patients (fifteen women, five men), and five traditional healers (four men, one woman) were interviewed. All participants were Afro-Colombians and indigenous people from Quibdó, Colombia, with a mean age of 62.38 years (men) and 53.40 years (women). The selection of medicinal plant sellers was based on their interest in participating in the research and their experience in cultivating and selling medicinal plants. Diabetic and/or obese patients were selected based on their interest in participating in the research and their use of medicinal plants as complementary treatments for their condition. Traditional healers were selected based on their interest in participating in the research, their reputation among patients, recognition by the plant sellers and interviewed patients, and the number of patients they have treated.

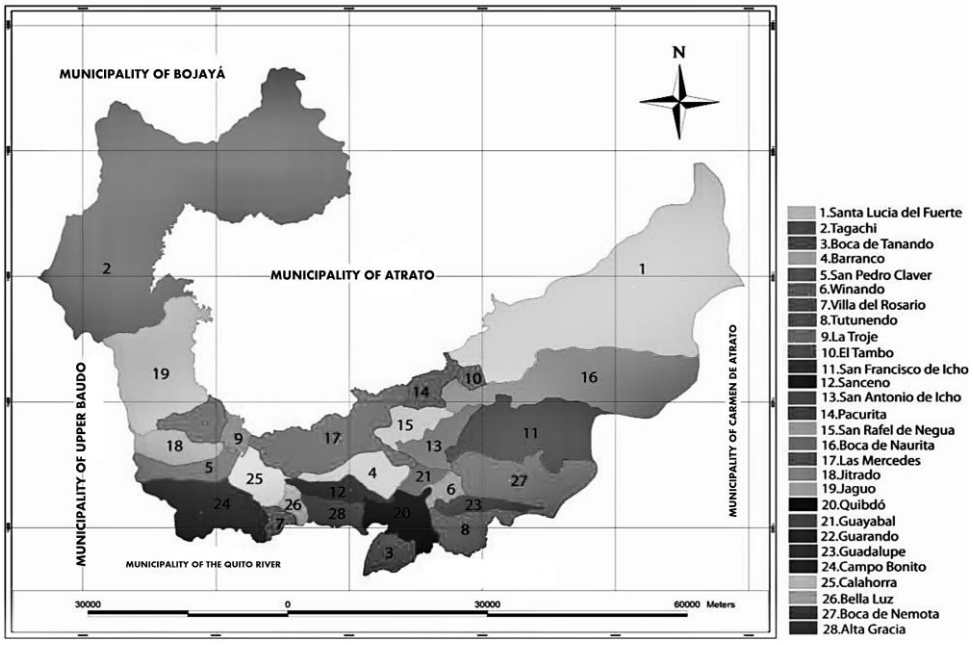

Figure 1. Study area, made from the official map of the mayor's office of Quibdó.

The questionnaire consisted of seventeen questions and aimed to gather general personal information. The main topics covered were: (1) plant name, (2) general plant description, (3) preparation method, (4) form of consumption, (5) duration of treatment, (6) symptoms relieved after consumption, (7) benefits, (8) recommendation for plant use, and (9) plant acquisition source. This questionnaire was specifically designed and utilized to calculate the use value (UV) of each medicinal plant used in ethnopharmacological treatments for diabetes and obesity. Through this process, a list of medicinal plants was compiled, and the collected data were analyzed using descriptive statistical methods. Equation (1) was employed to identify the most promising species [30,31]. The information obtained was compared with previous ethnobotanical studies conducted in the study area [32].

$$UVis = \sum Uis/Nis, \quad (1)$$

where U*is* is the number of uses mentioned for species (s) by the informant and N*is* is the number of events in which the informant cites a use for species (s).

2.4. Plant Material

The five plants with the highest use value were collected in September 2018 from wild populations around the town of Quibdó, Chocó, Colombia (5°41′0.78″ N, −76°35′15.4″ W). The plant material was identified by the Joaquín Antonio Uribe Herbarium (JAUM) and the National Herbarium of Colombia (COL), and a voucher specimen of *Artocarpus altilis* (Parkinson ex FAZorn) Fosberg. (JAUM 7556), *Vismia macrophylla* Kunth. (COL 205425), *Bauhinia picta* (Kunth) DC. (JAUM 91811), *Momordica balsamina* L. (COL 205423), and *Neurolaena lobata* (L.) R.Br. ex Cas. (COL 205424) were deposited in the corresponding herbarium.

2.5. Hydroalcoholic Extracts (HE)

Each of the five species (1 kg each) was subjected to air-drying at room temperature and subsequently mechanically pulverized. The pulverized material underwent extraction through maceration using a hydroalcoholic mixture (ethanol:water, 70:30) at a ratio of 1:4 (*w*/*v*) for one week, with solvent changes every 48 h. The resulting extract was then evaporated under reduced pressure and stored at 4 °C, protected from light, until analysis.

2.6. Digestive Enzyme Inhibition Assays

2.6.1. α-Glucosidase Inhibition Assay

The AG inhibitory activity of the extract, fractions, and isolated compounds was determined in 96-well microtiter plates by the method described previously [33]. Briefly, α-glucosidase from *Saccharomyces cerevisiae* (type I, lyophilized powder, ≥10 units/mg protein) was added to phosphate buffer (0.1 M, pH 7.2, BSA 1%) at 0.5 U/mL and 10 µL were mixed in 96-well microtiter plates containing 10 µL of different concentrations of the extract and fractions (400–12.5 µg/mL, DMSO solution, 2% v/v) or compounds tested (400–3.1 µM, DMSO solution, 2% v/v) at room temperature for 10 min. The reactions were initiated by the addition of 10 µL of 4-nitrophenyl-α-d-glucopyranoside (PNPG) at a concentration of 400 µM. The reaction mixture was incubated at 37 °C for 15 min in a final volume of 250 µL. Then, 0.2 M Na_2CO_3 (40 µL) was added to the incubation solution to stop the reaction, and absorbance was determined at 405 nm (for p-nitrophenol). Acarbose was used as a positive control (400–12.5 µg/mL).

$$\text{Inhibition rate}(\%) = \frac{\text{ABSnc} - \text{ABSsam}}{\text{ABSnc}} \times 100 \quad (2)$$

where ABSnc: absorbance of negative control at 405 nm (for p-nitrophenol), AB-Ssam: absorbance of the sample at 405 nm (for p-nitrophenol).

2.6.2. α-Amylase Inhibition Assay

The AA inhibitory activity was performed according to Ryu et al. [34], with some modifications. In brief, α-amylase from porcine pancreas (Type IV, lyophilized powder, ≥5 units/mg protein) was prepared in phosphate buffer (0.1 M, pH 7.2, BSA 1%) at 0.5 U/mL and 50 µL were mixed in 96-well microtiter plates with 50 µL of various concentrations of extracts and fractions (20.0–1.0 mg/mL, DMSO solution, 2% v/v), tested compounds (400–3.1 µM, DMSO solution, 2% v/v), or acarbose (20.0–1.0 mg/mL, DMSO solution, 2% v/v) at room temperature for 30 min. Reactions were initiated by the addition of 50 µL of starch (5%) and incubated for 60 min at 37 °C. Finally, 100 µL of 3,5-dinitro salicylic acid (DNS, 0.04 M) was added and heated for 10 min at 100 °C. After the reaction time, the absorbance at 540 nm was measured. In this essay, two reaction blanks were used: blank 1, which consisted of a mixture of DNS reagent, DMSO, and buffer; and blank 2, which consisted of a mixture of buffer, extracts and/or compounds at different concentrations, a 5% starch solution, and DNS reagent. All assays were performed in triplicate in two independent experiments. IC_{50} values were estimated by nonlinear regression analysis and the inhibition rate (%) was estimated using Equation (2).

2.6.3. Pancreatic Lipase Inhibition Assay

The PL inhibitory activity of the extract, fractions, and isolated compounds was determined in 96-well microtiter plates according to the previously described method [33]. In brief, pancreatic lipase from porcine pancreas (type II, lyophilized powder, ≥30–90 units/mg protein) was prepared in Tris-HCl buffer (0.1 M, pH 8.4, Tween 20 1%, BSA 1%) at 200 U/mL, and 30 µL of different concentrations of extract and fractions (600–12.5 µg/mL, DMSO solution) or tested compounds (600–3.1µM, DMSO solution) mixed at room temperature for 30 min, maintaining a 2% v/v concentration of DMSO per well. The reactions were initiated by the addition of 30 µL of 4-nitrophenyl butyrate at a concentration of 400 µM. The reaction mixture was incubated at 37 °C for 30 min in a final volume of 250 µL, and absorbance was determined at 405 nm (for p-nitrophenol). Orlistat was used as a positive control (600–12.5 µg/mL). The blank value was adjusted by adding a Tris-HCl buffer instead of the PL. All assays were performed in triplicate in three independent experiments. IC_{50} values were estimated by nonlinear regression analysis and the inhibition rate (%) was estimated using Equation (2).

2.7. Isolation of Bioactive Compounds from the Stem Bark of V. macrophylla

A total of 28 g of hydroalcoholic extract (HE) of *V. macrophylla* was fractionated by VLC using solvents of different polarity: n-hexane (3.68 g, yield = 13.16%), chloroform ($CHCl_3$) (2.58 g, yield = 9.21%), and ethyl acetate (EtOAc) (18.00 g, yield = 64.29%). The resulting fractions were tested as inhibitors of catalytic activity against PL, AA, and AG, establishing that the fractions of n-hexane and EtOAc were the ones with the better inhibitory activity. The n-hexane fraction (2.5 g) was subjected to VLC chromatography using a gradient system of n-hexane–EtOAc (100:0 to 0:100, v/v) to give eight fractions (n-hxF1–F8) after combining them according to their TLC profiles. The hx-F6 fraction (690 mg) was purified by FC using a gradient system of $CHCl_3$:MeOH (98:02 to 90:10, v/v), resulting in four subfractions (hx-F6.1–F6.4). Purification of the hx-F6.4 subfraction (118 mg) by FC using a gradient system $CHCl_3$:MeOH (95:5) and $CHCl_3$:MeOH (90:10) led to the isolation of compound 1 (10.0 mg, pale yellow amorphous solid). The EtOAc fraction (15 g) was subjected to VLC using a gradient system of CH_2Cl_2–MeOH (100:0 to 0:100, v/v) to give eight subfractions (EtOAc-F1–F8) after combining them according to their TLC profiles. The fraction EtOAc-F7 (859.5 mg) was purified by FC with CH_2Cl_2–EtOAc (90:10 to 70:30 v/v) to obtain 10 subfractions (EtOAc-F7.1–7.10). The fraction EtOAc-F-7.2 (23.9 mg) was purified by FC with CH_2Cl_2: EtOAc (95:5 to 90:10) purification, resulting in the isolation of two compounds: compound 2 (6.2 mg, white amorphous solid) and compound 3 (6.0 mg, white needles). The structural elucidation of isolated compounds was performed by NMR (1H, 13C, COSY, HMBC, and HMQC), and by comparison of data reported in the literature. Figure S1 shows the general purification scheme of compounds **1** to **3**.

2.8. Enzyme Kinetic and Inhibition Mechanism Assay

The K_m and V_{max} values of each enzyme were determined by spectrophotometric methods. Briefly, the enzyme solutions [E] were incubated with different concentrations of the substrates [S], α-glucosidase (5000–4.88 μM, [S]), and pancreatic lipase (2000–1.98 μM, [S]) following the protocol described above. Thus, K_m and V_{max} values for each enzyme were determined through the Michaelis–Menten equation (Equation (3)) using the statistical program GraphPad Prism 8.0 and Hyper32. The inhibition effect on enzyme kinetics was estimated by incubating the solutions [E + S] with different concentrations of the inhibitor [I] at IC_{50}*2, IC_{50}, and $IC_{50}/2$, and K_i values for each [I] were estimated through the Cheng–Prusoff equation (Equation (4)). The data obtained were plotted through equations of Lineweaver–Burk diagrams and the inhibition mechanisms were estimated as mixed and non-competitive.

$$V_0 = \frac{V_{max}[S]}{K_m[S]}, \quad (3)$$

$$K_i = \frac{IC_{50}}{1 + \frac{[S]}{K_m}}, \quad (4)$$

where V_0: initial velocity, V_{max}: maximal velocity, K_m: maximal velocity $\frac{1}{2}$, $[S]$: concentration of substrate, K_i: inhibition constant.

2.9. Molecular Docking

SeInteraction, docking, and binding analyses in 3D were performed using AutoDock4 (AD4), AutoDock Vina 1.1.2 (ADV), and Glide (Mae) software (Master Release-2016 from the Schrödinger platform) [35,36]. The crystallographic structures and their three-dimensional (3D) coordinates of the PL enzymes (PDB code: 1LPB, resolution of 2.4 Å) [37], AG (PDB code: 2QMJ, resolution of 1.9 Å) [36], and AA (PDB code: 4GQR, resolution of 1.2 Å) [38] were obtained from RCSB PDB (https://www.rcsb.org/, accessed on 9 May 2021) in complex with their respective ligands (inhibitors): methoxyundecylphosphinic acid (MUP), acarbose, and myricetin. The chemical structures (2D) of the ligands were processed by ChemDraw Professional. 16.0, obtaining the simplified molecular input line entry system

(SMILES) structures in its database. Finally, and based on the experimental data of the type of inhibition, the most probable binding sites of the ligands (1, 2, and 3) were evaluated, and the binding mode was analyzed and compared with the results obtained by each enzyme target. The Maestro academic software was used to generate 2D and 3D figures of the binding modes [38].

2.10. Statistical Analysis

Statistically significant differences in the biological effects of inhibitors (extracts, fractions, and compounds) were analyzed and compared using ANOVA, supplemented by Tukey HSD post hoc analysis. All reported data to correspond to the average of three repetitions ± standard deviation, and the statistical significance considered was $p < 0.05$.

3. Results and Discussion

3.1. Ethnopharmacology of Diabetes and Obesity in Chocó, Colombia

In this study, an ethnopharmacological survey was conducted among randomly selected medicinal plant sellers, traditional healers, and patients diagnosed with diabetes/obesity. Forty-five individuals agreed to participate in the study after being informed about its purpose and voluntarily expressing their intention to participate through informed consent. The ethnopharmacological survey served as the initial step in identifying the most used and recognized medicinal plants for ethnotherapeutic treatment of diabetes and obesity in the Colombian Pacific region. As a result, twenty-nine (29) plants from twenty-one (21) families were identified (Table 1). The relative importance of these plants in the treatment of diabetes/obesity was assessed using the use value equation (UV), a widely used index to quantify the relative significance of useful plants. The UV combines the frequency of species mentions with the number of uses mentioned per species and is often employed to highlight key species of interest [39,40]. Consequently, Artocarpus altilis (UV = 0.8), Momordica balsamina (UV = 0.72), Bauhinia picta (UV = 0.64), Neurolaena lobata (UV = 0.76), and Vismia macrophylla (UV = 0.64) were identified as prominent and crucial species in the preparation of natural remedies for diabetes/obesity treatment.

The results of the ethnopharmacological study agree with the data reported in previous studies carried out by García-Cossio [32], where approximately 20 years ago, the decoctions and infusions of the leaves of *A. altilis*, *B. picta*, and *M. balsamina* were the most used natural remedies for the treatment of diabetes and obesity in Quibdó (Chocó, Colombia). Likewise, these species have also been reported in Mexico, Panama, Guatemala, Pakistan, and some African countries as medicinal plants for the treatment of obesity and diabetes [37,39–44]. On the other hand, in our study, *V. macrophylla* and *N. lobata* are reported for the first time as medicinal plants to treat obesity and diabetes in the Colombian Pacific. However, *N. lobata* is also reported for the treatment of obesity in Guatemala and Mexico [45].

The five species with the most prominent UV values were selected to carry out a series of in vitro studies to develop experimental evidence on their therapeutic potential as inhibitors of target digestive enzymes with a fundamental role in the pathophysiology of diabetes and obesity. Table 2 shows the results of enzyme inhibition on AG, AA, and PL expressed as IC_{50} values for each hydroalcoholic herbal extract. As a results, we found that the hydroalcoholic extracts obtained from these five species inhibit the catalytic activity of the three digestive enzymes with IC_{50} values between 0.99 and 123.30 µg/mL on AG, 4.23 and 37.80 mg/mL on AA, and between 17.18 and 250.00 µg/mL on PL. This study reports for the first time the bioactivity of all extracts on AA and PL. The inhibitory effect on AG is reported for the first time for *V. macrophylla*, while for *N. lobata*, *M. balsamina*, *B. picta* and *A. altilis*, our results agree with previously reported data where the experimental conditions were similar [37,39–44]. The extracts obtained from the leaves and stem bark of *V. macrophylla* were the most promising on AG and AA, with the bioactivity of both extracts on AG being significantly higher than acarbose. On the other hand, on PL, the most active extracts were obtained from *N. lobata* (leaves), *M. balsamina* (leaves), and *V. macrophylla* (stem bark). However, all extracts evaluated were significantly less active than orlistat. The

results suggest that the hydroalcoholic extract obtained from the stem bark of *V. macrophylla* has multitarget potential to inhibit the digestive enzymes of interest. Therefore, this extract was selected to carry out a bio-guided fractionation study in search of identifying some bioactive constituents.

Table 1. List of species used for medicinal purposes (diabetes and obesity) in the Colombian pacific (Quibdó, Chocó).

Species	Family	Common Name	Used Part	FTP	TU	UV
Justicia chlorostachya	Acanthaceae	Insulina	Leaves	D and I	DM	0.48
Trichanthera gigantea	Acanthaceae	Quiebra barriga	Leaves	D and I	OB	0.52
Amaranthus sp.	Amarantaceae	Amaranto	Leaves	D	OB	0.56
Iresine herbstii	Amarantaceae	Escancel	Leaves	D and I	DM	0.52
Anacardium occidentale	Anacardiaceae	Mango	Leaves	D and I	OB and DM	0.48
Annona muricata	Annonaceae	Guanábana	Fruits and leaves	D and J	DM	0.48
Neurolaena lobata	Asteraceae	Venadillo	Whole plant	D	DM	0.76
Bidens pilosa	Asteraceae	Pacunga	Whole plant	D and I	DM	0.48
Spilanthes paniculata	Asteraceae	Botoncillo	Leaves	D	OB	0.52
Bauhinia picta	Fabaceae	Casco de vaca	Leaves	D and I	DM	0.64
Vismia macrophylla	Hypericaceae	Manchará	Leaves and bark	D and I	OB and DM	0.64
Momordica balsamina	Cucurbitaceae	Balsamina	Leaves	D	OB and DM	0.72
Kyllinga pumila	Cyperaceae	Espadilla	Leaves	D and I	OB and DM	0.56
Phaseolus vulgaris	Fabaceae	Frijol	Fruits and leaves	D and I	DM	0.48
Origanum vulgare	Lamiaceae	Orégano	Whole plant	D and I	DM	0.48
Plectranthus amboinicus	Lamiaceae	Orégano brujo	Whole plant	D and I	DM	0.48
Sida rhombifolia	Malvaceae	Escoba babosa	Leaves	D and I	OB and DM	0.48
Bellucia pentamera	Melastomataceae	Coronillo	Fruits and leaves	D and J	OB	0.52
Artocarpus altilis	Moraceae	Árbol del pan	Leaves	D	DM	0.80
Syzygium malaccense	Myrtaceae	Marañón	Fruits and leaves	D and J	OB and D	0.56
Eucalyptus globulus	Myrtaceae	Eucalipto	Leaves and bark	D and I	DM	0.48
Psidium guajava	Myrtaceae	Guayaba	Fruits and leaves	D and J	OB and DM	0.52
Averrhoa carambola	Oxalydaceae	Carambolo	Fruits and leaves	D and J	OB	0.48
Passiflora quadrangularis	Passifloraceae	Badea	Leaves	D and I	OB and DM	0.56
Peperomia pellucida	Piperaceae	Celedonia	Whole plant	D and I	OB	0.60
Scoparia dulcis	Plantaginaceae	Escubilla	Leaves	D and I	OB	0.48
Cymbopogon citratus	Poaceae	Limoncillo	Whole plant	D	DM	0.52
Physalis peruviana	Solanaceae	Uchuva	Fruits and leaves	D and I	DM	0.60
Pilea microphylla	Urticaceae	Cien piecitos	Whole plant	D	OB and DM	0.48

UV: use value, FTP: form of the traditional preparation, TU: therapeutic use. D: decoction, I: infusion, J: juice, OB: obesity, DM: type 2 diabetes.

Table 2. Inhibitory effect on AG, AA, and PL of herbal extracts with the highest UV in the treatment of diabetes and obesity in Chocó, Colombia.

Extracts	AG $IC_{50} \pm SD$ (µg/mL)	AA $IC_{50} \pm SD$ (mg/mL)	PL $IC_{50} \pm SD$ (µg/mL)
B. picta	35.80 ± 3.2	7.34 ± 0.36	64.28 ± 5.20
M. balsamina	123.30 ± 2.5	NA	22.85 ± 7.28 *
N. lobata	71.23± 1.8	37.80 ± 2.43	17.18 ± 2.55 *
A. altilis	55.07 ± 2.9	24.48 ± 1.50	30.46 ± 5.24
V. macrophylla stem bark	0.99 ± 0.12 **	5.61 ± 0.82	28.91 ± 2.10
V. macrophylla leaves	5.74 ± 1.55 *	4.23 ± 0.24	250.00 ± 5.40
[a] Acarbose	104.00 ± 2.9	0.80 ± 0.04 **	
[b] Orlistat			4.41 ± 2.04 *

IC_{50} values are expressed as mean ± standard deviation (SD), where $n = 3$ in three independent assays. AG: α-glucosidase, AA: α-amylase, PL: pancreatic lipase. [a, b], positive controls. NA: not active. * ($p < 0.001$) ** ($p < 0.0001$) statistically significant differences (Tukey HSD).

3.2. Phytochemical Study of the Stem Bark of V. macrophylla and Enzymatic Inhibition against PL, AA, and AG

To select the bioactive fractions for the phytochemical study obtained from the hydroalcoholic extract of *V. macrophylla*, the n-hexane, chloroform ($CHCl_3$), and ethyl acetate (EtOAc) were subjected to a study of the inhibitory effect on the catalytic activity of PL, AA,

and AG. Table 3 shows the IC_{50} values on PL, AA, and AG of the VLC fractions from *V. macrophylla* stem bark. These results indicate that the n-hexane fraction is the most active to inhibit the PL, while on AG and AA, the most active is the EtOAc fraction.

Table 3. Inhibitory effect on AG, AA, and PL of the hydroalcoholic extract and the fractions obtained from the stem bark of Vismia macrophylla.

Extracts/Fractions	AG $IC_{50} \pm SD$ (µg/mL)	AA $IC_{50} \pm SD$ (mg/mL)	PL $IC_{50} \pm SD$ (µg/mL)
V. macrophylla Stem bark HE	0.99 ± 0.21 ***	5.61 ± 0.82	28.91 ± 2.10 *
n-hexane fraction	NA	NA	9.37 ± 3.00 **
$CHCl_3$ fraction	3.47 ± 1.08 ***	6.80 ± 0.92	26.53 ± 5.38 *
EtOAc fraction	0.59 ± 0.10 ***	1.96 ± 0.62 **	68.84 ± 1.00
[a] Acarbose	104.00 ± 2.9	0.80 ± 0.04 ***	
[b] Orlistat			4.41 ± 2.04 **

IC_{50} values are expressed as mean ± standard deviation (SD), where n = 3 in three independent assays. HE: hydroalcoholic extract, AG: α-glucosidase, AA: α-Amylase, PL: pancreatic lipase., [a, b], positive controls. NA: inactive. * ($p < 0.05$) ** ($p < 0.001$) *** ($p < 0.0001$) statistically significant differences (Tukey HSD).

The phytochemical study carried out on the selected fractions from the stem bark of *V. macrophylla* led to the isolation of three bioactive compounds known as 5′-demethoxycadensin G **1,** *para*-hydroxybenzoic acid methyl ester **2,** and *para*-hydroxybenzoic acid butyl ester **3** (Figure 2). These compounds are reported for the first time for the stem bark of *V. macrophylla*. However, these secondary metabolites have been previously reported in species of the genus *Vismia* Vand. (Hypericaceae) and other species of the family such as *Cratoxylum* spp., *Hypericum* spp., *Garcinia* spp., and *Psorospermum* spp. [29,46,47]. Thus, compounds **2** and **3** have been reported as an antineoplastic agents, hepatoprotective, anti-inflammatory, antifungal, and antibacterial [47–49], while compound **1** has been reported as an antioxidant [50,51].

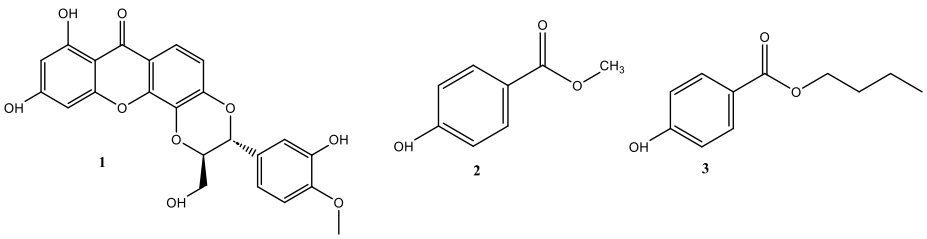

Figure 2. Structures of isolated compounds from the stem bark of *Vismia macrophylla* (Hypericaceae).

Compound 1: 5′-demethoxycadensin G, pale yellow amorphous solid, melting point (m.p.): 277–280 °C. ^{1}H-NMR ($CDCl_3$, 300 MHz) δ (ppm) 13.10 (s, 1H), 7.71 (d, J = 8.9 Hz, 1H,), 7.18 (d, J = 1.9 Hz, 1H), 7.03 (dd, J = 1.9 Hz, 8.1 Hz, 1H), 7.01 (d, J = 8.9 Hz, 1H), 6.91 (d, J = 8.1 Hz, 1H), 6.47 (d, J = 2.1 Hz, 1H), 6.27 (d, J = 2.1 Hz, 1H), 5.22 (d, J = 7.9 Hz, 1H), 4.31 (ddd, J = 7.9, 3.8, 2.4 Hz, 1H), 3.88 (s, 3H), 3.92 (dd, J = 12.6, 3.8 Hz, 1H), 3.62 (dd, J = 12.6, 2.4 Hz, 1H). APT (75 MHz, $CDCl_3$): δ (ppm) 181.7 (C-9), 167.4 (C-3), 165.7 (C-1), 159.7 (C-4a), 151.3 (C-6), 149.6 (C-3′), 149.4 (C-4′), 148.1 (C-4b), 133.9 (C-8a), 129.2 (C-1′), 122.7 (C-6′), 118.8 (C-8), 116.9 (C-5′), 116.4 (C-5), 115.5 (C-7), 113.1 (C-2′), 104.2 (C-9a), 100.2 (C-2), 95.9 (C-4), 80.6 (C-8′), 78.9 (C-7′), 62.5 (C-9′), 57.4 (C-3′) (Figures S2, S3 and S8). The spectroscopic data were consistent with those reported in the literature for 5′-demethoxycadensin G [50,52].

Compound 2: para-hydroxybenzoic acid methyl ester: white amorphous solid, melting point (m.p.): 130–131 °C. ^{1}H-NMR ($CDCl_3$, 300 MHz) δ (ppm) 7.88 (d, J = 8.5 Hz, 2H), 6.81 (d, J = 8.4 Hz, 2H), 3.82 (s, 3H). APT (75 MHz, $CDCl_3$): δ (ppm) 167.4 (C-1), 160.3 (C-2), 132.1 (C-3 and C-7), 122.5 (C-5), 115.4 (C-4 and C-6) and 52.2 (C-1′) (Figures S4 and S5). The spectroscopic data were consistent with those reported in the literature for para-hydroxybenzoic acid methyl ester [53].

Compound 3: para-hydroxybenzoic acid butyl ester, white needles, melting point (m.p.): 69–71 °C. ^{1}H-NMR ($CDCl_3$, 300 MHz) δ (ppm) 7.88 (d, J = 8.5 Hz, 2H), 6.81 (d,

J = 8.4 Hz, 2H), 4.23 (t, J = 6.5 Hz, 2H), 1.67 (m, 2H), 1.40 (dq, J = 14.2, 7.3 Hz, 2H) and 0.90 (t, J = 7.3 Hz, 3H). APT (75 MHz, $CDCl_3$): δ (ppm) 167.0 (C-1), 160.2 (C-2), 132.0 (C-3 and C-7), 122.8 (C-5), 115.3 (C-4 and C-6), 64.95 (C-1′), 30.9 (C-2′), 19.4 (C-3′) and 13.9 (C-4′) (Figures S6 and S7). The spectroscopic data were consistent with those reported in the literature for para-hydroxybenzoic acid butyl ester [54,55].

Table 4 shows the IC_{50} values, inhibition constant values (Ki), and the inhibition mechanism estimated for compounds **1–3** on AA, AG, and PL. Compounds **1–3** do not inhibit AA at the tested concentrations. The compounds derived from para-hydroxybenzoic acid, **2** and **3,** have a significant inhibitory effect ($p < 0.001$) on PL, but not on AG, while compound **1** causes inhibition in the catalytic activity of PL (IC_{50} = 187.50 ± 0.33 μM, Ki = 187.50 μM) and AG (IC_{50} = 164.30 ± 0.11 μM, Ki = 131.70 μM). This is the first report of the inhibitory activity of these compounds as natural bioactive inhibitors of digestive enzymes of interest in the treatment of obesity and diabetes.

Table 4. Inhibition of AG and PL by compounds **1–3**.

Compounds	α-Glucosidase			Pancreatic Lipase		
	IC_{50} (μM)	k_i μM	Inhibitor Type	IC_{50} (μM)	k_i μM	Inhibitor Type
1	164.30 ± 0.11 *	131.70	C	187.50 ± 0.33	187.50	M
2	>400	-	-	28.50 ± 4.07 *	10.60	NC
3	>400	-	-	10.15 ± 3.42 **	5.31	NC
Acarbose	315.20 ± 3.27	57.50	C	-		-
Orlistat	-			0.67 ± 0.04 ***	0.24	II

The evaluated concentration was in the range of 3.31–400 μM. These results are expressed as the mean of three replicates (n = 3) ± SD, in three independent assays. -: Inactive. Inhibitor type, II: irreversible inhibitor, C: competitive, NC: non-competitive. * ($p < 0.05$) ** ($p < 0.001$) *** ($p < 0.0001$) statistically significant differences (Tukey HSD).

Compound **1** was characterized as a moderate PL inhibitor characterizing itself as a mixed-type inhibitor that has a lower affinity for the enzyme than the substrate used in the bioassays. Xanthone and anthraquinone-type compounds have been widely reported as potent inhibitors of pancreatic lipase [17,56]. On AG, compound **1** was twice as active as the acarbose positive control. The Lineweaver–Burk plot analysis estimated experimentally on AG shows that the inhibitory effect of **1** is characterized by mixed-type inhibition. The treatment of AG with this tetra-oxygenated xantholignoid significantly increases the K_m of the enzyme, while due to its mixed-type inhibition mechanism (Figure 3), V_{max} tends to decrease, requiring a higher concentration of the substrate to decrease the inhibitory effect. In contrast, the acarbose does not alter the V_{max} of AG, but the K_m of the enzyme significantly increases, a characteristic effect of the reversible competitive inhibitors [30,31]. The protein–ligand docking analysis and the visualization for AG and compound **1** were also guided by the experimental type of inhibition. The binding energy of **1** (−8.2 kcal/mol) and blind molecular docking did not show interactions with the catalytic triad formed by polar amino acid residues Asp203, Asp327, and Asp443. However, the aromatic ring with oxygenating groups of **1** is oriented towards the catalytic pocket and forms hydrophobic interactions with Trp406, while the carbonyl group of B ring forms hydrophilic interactions with Arg202. The xanthone-type compounds have been reported as promising bioactive molecules to treat obesity and diabetes [56,57]. In a comprehensive review about xanthones as inhibitors of AG activity, Santos et al. [57] report more than 280 bioactive analogs against this therapeutic target. According to this paper, the presence of a hydroxyl group located at C-1 or C-8 seems to be important for the high inhibitory activity against AG, while the steric hindrance produced by the glycoside residue at position C-7 lowers the inhibitory activity. Likewise, Liu et al. [58] report that xanthone-type compounds belong to competitive, noncompetitive, and mixed inhibitors and induce a loss in the α-helix content of the secondary structure of AG, while the docking simulation revealed the existence of multiple binding modes in which polyhydroxy groups and expanded aromatic rings acted as two key pharmacophores to form H-bonding and π–π stacking interactions with AG

(Figure 3). These experimental values agree with the Cheng–Prusoff hypothesis for this type of inhibitor [59]. Therefore, the inhibitory effect could be explained by the ability of the inhibitor to prevent the catalysis caused by the enzyme, regardless of whether the substrate is bound or not, i.e., this type of inhibitor can interact with both the free enzyme [E] and with the enzyme/substrate complex [ES] with the same affinity [60]. Although it is possible that both compounds can bind to the active site of the enzyme, this type of inhibition generally results from an allosteric effect where the inhibitor binds to another site that is not properly the active site, but this binding could block or change the affinity of the enzyme for the substrate [S] [61].

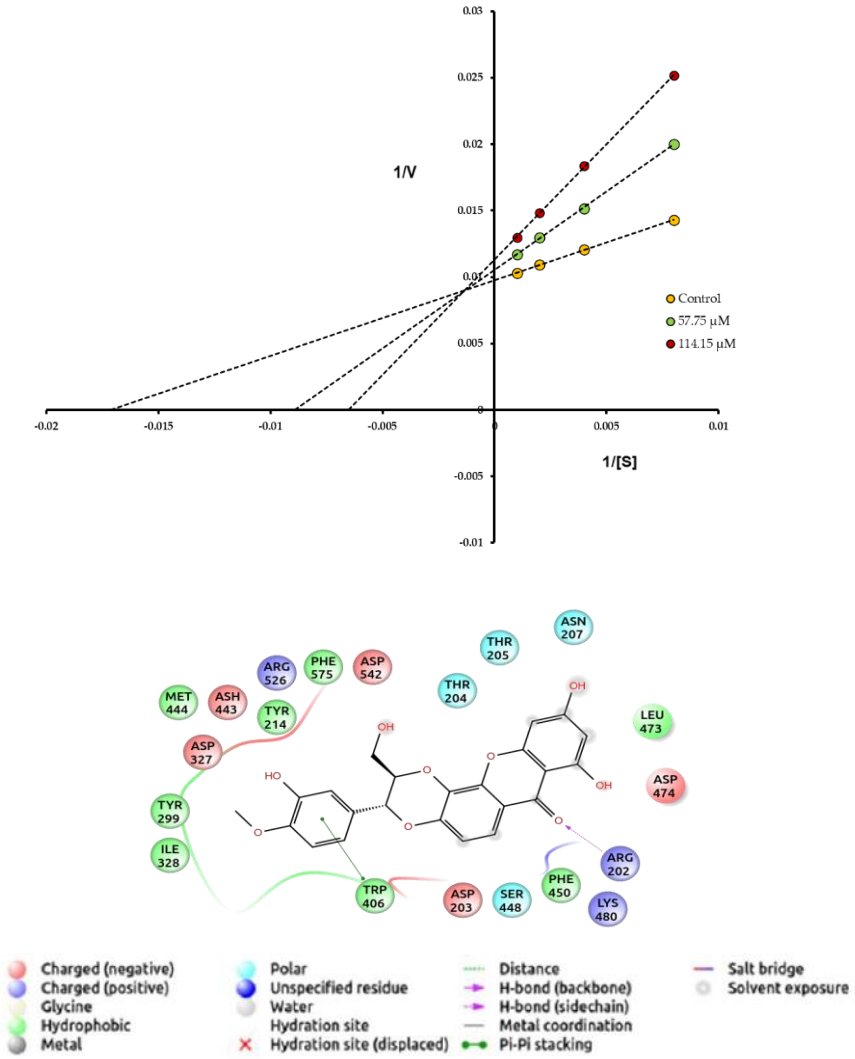

Figure 3. Mechanism of inhibition and Lineweaver–Burk plot of compound **1** on AG. Docked pose of compound **1** on AG (code, PDB-2QMJ). Maestro 2022-1 for compound **1**.

Analyzing the IC_{50} values for **2** and **3,** it was found that the inhibitory effect on PL was increased with the size of the carbon chain of the compounds, with butyl (C_4H_9) derivative being three times more active than its methylated counterpart (CH_3), although its inhibitory effects were significantly ($p < 0.05$) lower than orlistat. The treatment of PL with these compounds changes the V_{max} of the enzyme but does not alter the K_m, which tends to be equal despite the different concentrations of the inhibitor. Lineweaver–Burk plot analysis estimated experimentally for the most active compounds on PL shows that the inhibitory effect of **2** and **3** is characterized by noncompetitive-type inhibition (Figure 4). The protein–ligand docking analysis for PL and compounds **2** and **3** was carried out with AutoDock Vina [62] and the visualization with Free Maestro [63]. The binding

site selection (orthosteric or allosteric) was guided by the experimental type of inhibition (Table 4). The binding energies of **2** (−11.5 kcal/mol) and **3** (−12.0 kcal/mol) and blind molecular docking show interactions with the catalytic triad. The aromatic ring of **3** shows hydrophobic interactions between His151 and His263, while the free hydroxyl group shows hydrophilic interactions with Asp79 and Gln76 (Figure 4A), whereas **2** only shows hydrophilic interactions through the oxygen of the ester group with Ser152. However, as mentioned above, **3** is twice more active than **2**, demonstrating the fundamental role of Ser152 in inhibiting the catalytic activity of PL. According to Sankar and Engels [64], the docked g-score of orlistat on PL-1LPB was −9.47 and it showed key hydrophilic interactions with Phe77, Leu153, and Tyr114. In this study, it was observed that the hydrogen bond between the carbonyl atoms of the ester group and the amino acid residue Phe77 was invariably presented in all the evaluated compounds including the standard drug orlistat. Likewise, in our experimental evidence, molecular interactions with the Phe77 residue were also observed for the most bioactive compounds on PL. However, the most important interactions for these compounds were shown between the oxygen of the carbonyl group attached to ring B with Ser152; the essential nucleophilic residue for catalysis that is in the N-terminal domain and plays a critical role in the lipase−lipid interactions together with the β5′ loop [65,66].

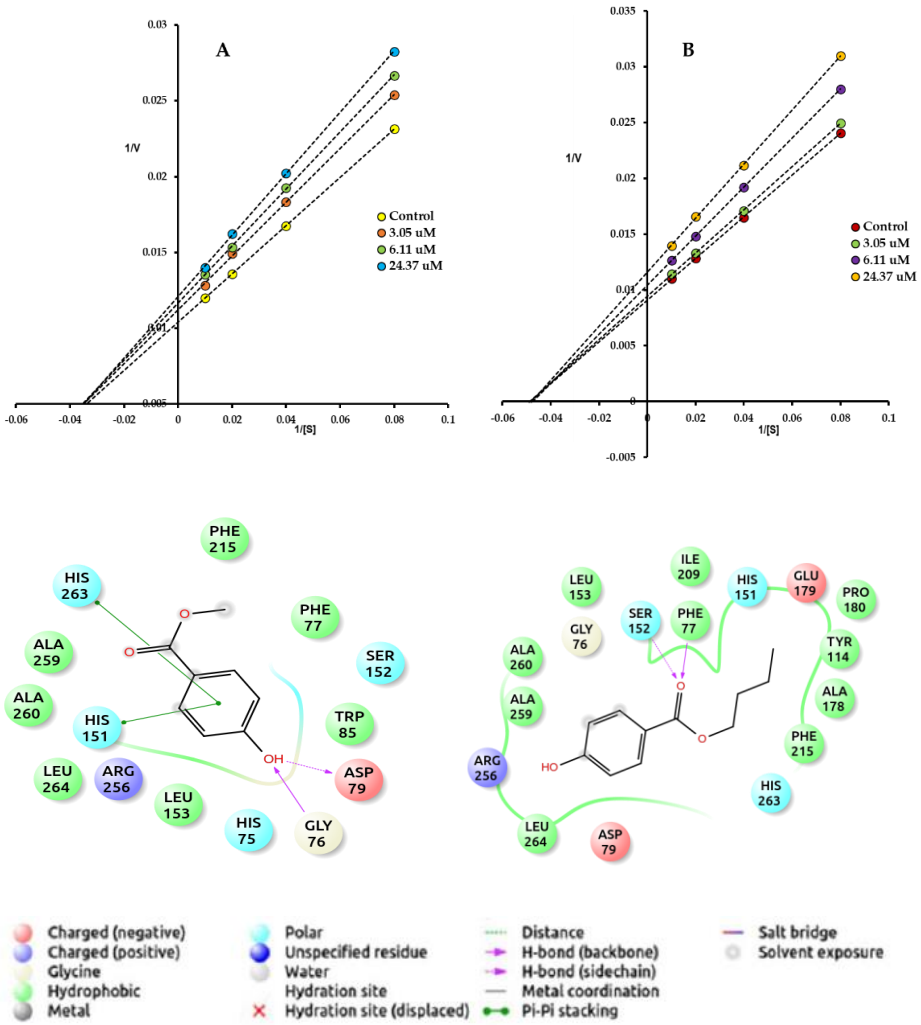

Figure 4. Mechanism of inhibition and Lineweaver–Burk plot of compounds **2** and **3** on PL. (**A**) Compound **2** (noncompetitive-type inhibition). (**B**) Compound **3** (noncompetitive-type inhibition). Docked pose of compounds **2** and **3** on PL (code, PDB-1LPB) (**A**) Maestro 2022-1 for compound **2**. (**B**) Maestro 2022-1 for compound **3**.

4. Conclusions

The present study significantly contributes to the field of ethnopharmacology in Chocó, Colombia, specifically in the treatment of diabetes and obesity. The identification of *V. macrophylla*, *N. lobata*, *A. altilis*, *M. balsamina*, and *B. picta* as the most valuable species based on their traditional usage provides valuable insights. Furthermore, the study successfully identifies bioactive compounds within *V. macrophylla* that exhibit notable effects on the digestive enzymes pancreatic lipase (PL) and α-glucosidase (AG). These findings emphasize the potential of *V. macrophylla* and its xantholignoid compound as promising multitarget inhibitors of digestive enzymes, thereby making a substantial contribution to the development of treatments for obesity and type 2 diabetes. Moreover, the study highlights the promising approach of combining ethnopharmacological methods, bio-guided phytochemical studies, and computational tools as an effective strategy for elucidating the therapeutic properties of medicinal plants.

Supplementary Materials: The following supporting information can be downloaded at: https://www.mdpi.com/article/10.3390/scipharm91040049/s1, and correspond to fractionation scheme of the hydroalcoholic extract of the stem bark of *Vismia macrophylla* (Figure S1), ^{1}H-NMR and APT spectra of compounds **1** to **3** (Figures S2–S7), the absolute configuration of 5′-demethoxycadensin G (3) (Figure S8).

Author Contributions: Conceptualization, K.P.L.-M., J.A.P.-R. and O.J.P.-L.; methodology, K.P.L.-M.; formal analysis, K.P.L.-M., J.A.P.-R. and O.J.P.-L.; investigation, K.P.L.-M.; data curation and interpretation, K.P.L.-M., J.A.P.-R. and O.J.P.-L.; original draft preparation, K.P.L.-M., J.A.P.-R. and O.J.P.-L.; supervision, J.A.P.-R. and O.J.P.-L.; funding acquisition, J.A.P.-R. and O.J.P.-L. All authors contributed to the writing of the manuscript. All authors have read and agreed to the published version of the manuscript.

Funding: This research was funded by Pontificia Universidad Javeriana (ID PPTA 6460) and Universidad Nacional de Colombia (ID 42562), announcement "VRI-04_PROF_PHD_COR2".

Institutional Review Board Statement: The study was conducted according to the Declaration of Helsinki and approved by the Ethics Committee of Pontificia Universidad Javeriana (Minutes No. 17 of 18 September 2014).

Informed Consent Statement: Informed consent was obtained from all subjects involved in the study.

Data Availability Statement: Not applicable.

Acknowledgments: The authors extend their gratitude to the research groups, GIFUJ belonging to the Pontificia Universidad Javeriana and QUIPRONAB belonging to the Universidad Nacional de Colombia, for their collaboration in the development of the research.

Conflicts of Interest: The authors declare no conflict of interest.

References

1. Lin, X.; Li, H. Obesity: Epidemiology, Pathophysiology, and Therapeutics. *Front. Endocrinol.* **2021**, *12*, 706978. [CrossRef] [PubMed]
2. Avgerinos, K.I.; Spyrou, N.; Mantzoros, C.S.; Dalamaga, M. Obesity, and Cancer Risk: Emerging Biological Mecha-nisms and Perspectives. *Metabolism* **2019**, *92*, 121–135. [CrossRef]
3. Piché, M.-E.; Tchernof, A.; Després, J.-P. Obesity Phenotypes, Diabetes, and Cardiovascular Diseases. *Circ. Res.* **2020**, *126*, 1477–1500. [CrossRef] [PubMed]
4. Lobstein, T.; Brinsden, H.; Neveux, M. World Obesity Atlas. 2022. Available online: https://policycommons.net/artifacts/2266990/world_obesity_atlas_2022_web/3026660/?utm_medium=email&utm_source=transaction (accessed on 1 April 2023).
5. Aras, M.; Tchang, B.G.; Pape, J. Obesity and Diabetes. *Nurs. Clin. N. Am.* **2021**, *56*, 527–541. [CrossRef] [PubMed]
6. Khan, M.A.B.; Hashim, M.J.; King, J.K.; Govender, R.D.; Mustafa, H.; Al Kaabi, J. Epidemiology of Type 2 Diabetes—Global Burden of Disease and Forecasted Trends. *J. Epidemiol. Glob. Health* **2020**, *10*, 107–111. [CrossRef]
7. Atlas, I.D. IDF Atlas 10th Edition, International Diabetes Federation. IDF Diabetes Atlas. 2021. Available online: https://fmdiabetes.org/wp-content/uploads/2022/01/IDF_Atlas_10th_Edition_2021-comprimido.pdf (accessed on 1 April 2023).

8. Sukhdev, S.; Bhupender, S.; Singh, K.S. Pharmacotherapy & Surgical Interventions Available for Obesity Manage-ment and Importance of Pancreatic Lipase Inhibitory Phytomolecules as Safer Anti-Obesity Therapeutics. *Mini Rev. Med. Chem.* **2017**, *17*, 371–379. [CrossRef]
9. Inthongkaew, P.; Chatsumpun, N.; Supasuteekul, C.; Kitisripanya, T.; Putalun, W.; Likhitwitayawuid, K.; Sritu-larak, B. α-Glucosidase and Pancreatic Lipase Inhibitory Activities and Glucose Uptake Stimulatory Effect of Phenolic Compounds from Dendrobium Formosum. *Rev. Bras. Farmacogn.* **2017**, *27*, 480–487. [CrossRef]
10. Hamden, K.; Mnafgui, K.; Amri, Z.; Aloulou, A.; Elfeki, A. Inhibition of Key Digestive Enzymes Related to Diabetes and Hyperlipidemia and Protection of Liver-Kidney Functions by Trigonelline in Diabetic Rats. *Sci. Pharm.* **2013**, *81*, 233–246. [CrossRef]
11. Kato-Schwartz, C.G.; de Sá-Nakanishi, A.B.; Guidi, A.C.; Gonçalves, G.D.A.; Bueno, F.G.; Zani, B.P.M.; de Mello, J.C.P.; Bueno, P.S.A.; Seixas, F.A.V.; Bracht, A.; et al. Carbohydrate Digestive Enzymes Are Inhibited by Poincianella Plu-viosa Stem Bark Extract: Relevance on Type 2 Diabetes Treatment. *Clin. Phytosci.* **2020**, *6*, 31. [CrossRef]
12. Lebovitz, H.E. alpha-Glucosidase inhibitors. *Endocrinol. Metab. Clin. N. Am.* **1997**, *26*, 539–551. [CrossRef]
13. Gromova, L.V.; Polozov, A.S.; Savochkina, E.V.; Alekseeva, A.S.; Dmitrieva, Y.V.; Kornyushin, O.V.; Gruzdkov, A.A. Effect of Type 2 Diabetes and Impaired Glucose Tolerance on Digestive Enzymes and Glucose Absorption in the Small Intestine of Young Rats. *Nutrients* **2022**, *14*, 385. [CrossRef]
14. Kaur, N.; Kumar, V.; Nayak, S.K.; Wadhwa, P.; Kaur, P.; Sahu, S.K. Alpha-amylase as molecular target for treatment of diabetes mellitus: A comprehensive review. *Chem. Biol. Drug Des.* **2021**, *98*, 539–560. [CrossRef]
15. Pilitsi, E.; Farr, O.M.; Polyzos, S.A.; Perakakis, N.; Nolen-Doerr, E.; Papathanasiou, A.-E.; Mantzoros, C.S. Pharma-cotherapy of Obesity: Available Medications and Drugs under Investigation. *Metabolism* **2019**, *92*, 170–192. [CrossRef] [PubMed]
16. Liu, T.T.; Liu, X.T.; Chen, Q.X.; Shi, Y. Lipase Inhibitors for Obesity: A Review. *Biomed. Pharmacother.* **2020**, *128*, 110314. [CrossRef]
17. Rajan, L.; Palaniswamy, D.; Mohankumar, S.K. Targeting obesity with plant-derived pancreatic lipase inhibitors: A comprehensive review. *Pharmacol. Res.* **2020**, *155*, 104681. [CrossRef]
18. Hou, X.D.; Ge, G.B.; Weng, Z.M.; Dai, Z.R.; Leng, Y.H.; Ding, L.L.; Jin, L.L.; Yu, Y.; Cao, Y.F.; Hou, J. Natural constituents from Cortex Mori Radicis as new pancreatic lipase inhibitors. *Bioorg. Chem.* **2018**, *80*, 577–584. [CrossRef]
19. Reed, J.; Bain, S.; Kanamarlapudi, V. A Review of Current Trends with Type 2 Diabetes Epidemiology, Aetiology, Pathogenesis, Treatments and Future Perspectives. Diabetes Metab. *Syndr. Obes. Targets Ther.* **2021**, *14*, 3567–3602. [CrossRef]
20. Quispe, Y.N.G.; Hwang, S.H.; Wang, Z.; Zuo, G.; Lim, S.S. Screening In Vitro Targets Related to Diabetes in Herbal Extracts from Peru: Identification of Active Compounds in *Hypericum laricifolium* Juss. by Offline High-Performance Liquid Chromatography. *Int. J. Mol. Sci.* **2017**, *18*, 2512. [CrossRef]
21. Jugran, A.K.; Rawat, S.; Devkota, H.P.; Bhatt, I.D.; Rawal, R.S. Diabetes and Plant-Derived Natural Products: From Ethnopharma-cological Approaches to Their Potential for Modern Drug Discovery and Development. *Phytother. Res. PTR* **2021**, *35*, 223–245. [CrossRef]
22. Atanasov, A.G.; Zotchev, S.B.; Dirsch, V.M.; Orhan, I.E.; Banach, M.; Rollinger, J.M.; Barreca, D.; Weckwerth, W.; Bauer, R.; Bayer, E.A.; et al. Natural Products in Drug Discovery: Advances and Opportunities. *Nat. Rev. Drug Discov.* **2021**, *20*, 200–216. [CrossRef]
23. Shi, Y.; Burn, P. Lipid Metabolic Enzymes: Emerging Drug Targets for the Treatment of Obesity. *Nat. Rev. Drug Discov.* **2004**, *3*, 695–710. [CrossRef]
24. Lunagariya, N.A.; Patel, N.K.; Jagtap, S.C.; Bhutani, K.K. Inhibitors of Pancreatic Lipase: State of the Art and Clini-cal Perspectives. *EXCLI J.* **2014**, *13*, 897–921. [PubMed]
25. Huo, P.-C.; Hu, Q.; Shu, S.; Zhou, Q.-H.; He, R.-J.; Hou, J.; Guan, X.-Q.; Tu, D.-Z.; Hou, X.-D.; Liu, P.; et al. Design, Synthesis and Biological Evaluation of Novel Chalcone-like Compounds as Potent and Reversible Pancreatic Lipase Inhibitors. *Bioorg. Med. Chem.* **2021**, *29*, 115853. [CrossRef]
26. Alhakamy, N.A.; Mohamed, G.A.; Fahmy, U.A.; Eid, B.G.; Ahmed, O.A.A.; Al-Rabia, M.W.; Khedr, A.I.M.; Nasrul-lah, M.Z.; Ibrahim, S.R.M. New Alpha-Amylase Inhibitory Metabolites from Pericarps of Garcinia Mangostana. *Life* **2022**, *12*, 384. [CrossRef]
27. Tundis, R.; Loizzo, M.R.; Menichini, F. Natural Products as Alpha-Amylase and Alpha-Glucosidase Inhibitors and Their Hypoglycaemic Potential in the Treatment of Diabetes: An Update. *Mini Rev. Med. Chem.* **2010**, *10*, 315–331. [CrossRef]
28. Chande, A.T.; Rowell, J.; Rishishwar, L.; Conley, A.B.; Norris, E.T.; Valderrama-Aguirre, A.; Medina-Rivas, M.A.; Jordan, I.K. Influence of Genetic Ancestry and Socioeconomic Status on Type 2 Diabetes in the Diverse Colombian Pop-ulations of Chocó and Antioquia. *Sci. Rep.* **2017**, *7*, 17127. [CrossRef]
29. Cruz, E.C.; Andrade-Cetto, A. Ethnopharmacological Field Study of the Plants Used to Treat Type 2 Diabetes among the Cakchiquels in Guatemala. *J. Ethnopharmacol.* **2015**, *159*, 238–244. [CrossRef]
30. Jenis, J.; Baiseitova, A.; Yoon, S.H.; Park, C.; Kim, J.Y.; Li, Z.P.; Lee, K.W.; Park, K.H. Competitive α-Glucosidase In-hibitors, Dihydrobenzoxanthones, from the Barks of Artocarpus Elasticus. *J. Enzym. Inhib. Med. Chem.* **2019**, *34*, 1623–1632. [CrossRef]
31. Li, Y.; Zhang, X.; Wang, R.; Han, L.; Huang, W.; Shi, H.; Wang, B.; Li, Z.; Zou, S. Altering the Inhibitory Kinetics and Molecular Conformation of Maltase by Tangzhiqing (TZQ), a Natural α-Glucosidase Inhibitor. *BMC Complement. Med. Ther.* **2020**, *20*, 350. [CrossRef]
32. García-Cossio, F.; Terán, J.M.; Mena, X.B.; Palacios, V.M.; Mena, W.R.; Palacios, O.P. La Diabetes en Quibdó y su tratamiento. *Rev. Inst. Univ. Tecnológica Chocó* **2003**, *18*, 16–21.

33. Cardozo-Muñoz, J.; Cuca-Suárez, L.E.; Prieto-Rodríguez, J.A.; Lopez-Vallejo, F.; Patiño-Ladino, O.J. Multitarget Action of Xanthones from Garcinia Mangostana against α-Amylase, α-Glucosidase and Pancreatic Lipase. *Molecules* **2022**, *27*, 3283. [CrossRef] [PubMed]
34. Ryu, H.W.; Cho, J.K.; Curtis-Long, M.J.; Yuk, H.J.; Kim, Y.S.; Jung, S.; Kim, Y.S.; Lee, B.W.; Park, K.H. α-Glucosidase Inhibition and Antihyperglycemic Activity of Prenylated Xanthones from Garcinia Mangostana. *Phytochemistry* **2011**, *72*, 2148–2154. [CrossRef] [PubMed]
35. Van Tilbeurgh, H.; Sarda, L.; Verger, R.; Cambillau, C. Structure of the Pancreatic Lipase-Procolipase Complex. *Nature* **1992**, *359*, 159–162. [CrossRef]
36. Sim, L.; Quezada-Calvillo, R.; Sterchi, E.E.; Nichols, B.L.; Rose, D.R. Human Intestinal Maltase-Glucoamylase: Crystal Structure of the N-Terminal Catalytic Subunit and Basis of Inhibition and Substrate Specificity. *J. Mol. Biol.* **2008**, *375*, 782–792. [CrossRef]
37. Zenderland, J.; Hart, R.; Bussmann, R.; Zambrana, N.; Sikharulidze, S.; Kikodze, D.; Tchelidze, D.; Khutsishvili, M.; Batsatsashvili, K. The Use of "Use Value": Quantifying Importance in Ethnobotany. *Econ. Bot.* **2019**, *73*, 293–303. [CrossRef]
38. Williams, L.K.; Li, C.; Withers, S.G.; Brayer, G.D. Order and Disorder: Differential Structural Impacts of Myricetin and Ethyl Caffeate on Human Amylase, an Antidiabetic Target. *J. Med. Chem.* **2012**, *55*, 10177–10186. [CrossRef]
39. Friesner, R.A.; Banks, J.L.; Murphy, R.B.; Halgren, T.A.; Klicic, J.J.; Mainz, D.T.; Repasky, M.P.; Knoll, E.H.; Shelley, M.; Perry, J.K.; et al. Glide: A New Approach for Rapid, Accurate Docking and Scoring. 1. Method and Assessment of Docking Accuracy. *J. Med. Chem.* **2004**, *47*, 1739–1749. [CrossRef]
40. Preto, J.; Gentile, F. Assessing and Improving the Performance of Consensus Docking Strategies Using the DockBox Package. *J. Comput. Aided Mol. Des.* **2019**, *33*, 817–829. [CrossRef]
41. Hussain, H.; Hussain, J.; Al-Harrasi, A.; Saleem, M.; Green, I.R.; van Ree, T.; Ghulam, A. Chemistry and Biology of Genus Vismia. *Pharm. Biol.* **2012**, *50*, 1448–1462. [CrossRef]
42. Andrade-Cetto, A.; Heinrich, M. From the Field into the Lab: Useful Approaches to Selecting Species Based on Local Knowledge. *Front. Pharmacol.* **2011**, *2*, 20. [CrossRef]
43. Andrade-Cetto, A.; Cruz, E.C.; Cabello-Hernández, C.A.; Cárdenas-Vázquez, R. Hypoglycemic Activity of Medici-nal Plants Used among the Cakchiquels in Guatemala for the Treatment of Type 2 Diabetes. *Evid.-Based Complement. Altern. Med. ECAM* **2019**, *2019*, 2168603. [CrossRef]
44. Dej-Adisai, S.; Pitakbut, T. Determination of A-Glucosidase Inhibitory Activity from Selected Fabaceae Plants. *Pak. J. Pharm. Sci.* **2015**, *28*, 1679–1683.
45. Mukesh, S.; Sikarwar, B.H. Pharmacognostical, Phytochemical and Total Phenolic Content of Artocarpus Altilis (Parkinson) Fosberg Leaves. *J. Appl. Pharm. Sci.* **2015**, *5*, 94–100.
46. Momina, S.; Rani, V. In Vitro Studies on α-Amylase and α-Glucosidase Inhibitory Activity of Some Bioactive Ex-tracts. *J. Young Pharm.* **2020**, *12*, s72–s75. [CrossRef]
47. Haber, S.L.; Awwad, O.; Phillips, A.; Park, A.E.; Pham, T.M. Garcinia Cambogia for Weight Loss. *Am. J. Health-Syst. Pharm. AJHP Off. J. Am. Soc. Health-Syst. Pharm.* **2018**, *75*, 17–22. [CrossRef] [PubMed]
48. Xiao, C.-Y.; Mu, Q.; Gibbons, S. The Phytochemistry and Pharmacology of Hypericum. *Prog. Chem. Org. Nat. Prod.* **2020**, *112*, 85–182. [CrossRef] [PubMed]
49. Vizcaya, M.; Morales, A.; Rojas, J.; Nunez, R. A Review on the Chemical Composition and Pharmacological Activi-ties of Vismia Genus (Guttiferae). *Bol. Latinoam. Caribe Plantas Med. Aromat.* **2012**, *11*, 12–34.
50. Boonnak, N.; Khamthip, A.; Karalai, C.; Chantrapromma, S.; Ponglimanont, C.; Kanjana-Opas, A.; Tewtrakul, S.; Chantrapromma, K.; Fun, H.K.; Kato, S. Nitric Oxide Inhibitory Activity of Xanthones from the Green Fruits of Cratoxylum Formosum ssp. *Pruniflorum. Aust. J. Chem.* **2010**, *63*, 1550–1556. [CrossRef]
51. Sim, W.C.; Ee, G.C.L.; Lim, C.J.; Sukari, M.A. Cratoxylum Glaucum and Cratoxylum Arborescens (Guttiferae)-Two Potential Source of Antioxidant Agents. *Asian J. Chem.* **2011**, *23*, 569–572.
52. Sia, G.-L.; Bennett, G.J.; Harrison, L.J.; Sim, K.-Y. Minor Xanthones from the Bark of Cratoxylum Cochinchinense. *Phytochemistry* **1995**, *38*, 1521–1528. [CrossRef]
53. Tian, J.-K.; Sun, F.; Cheng, Y.-Y. Chemical Constituents from the Roots of Ranunculus Ternatus. *J. Asian Nat. Prod. Res.* **2006**, *8*, 35–39. [CrossRef] [PubMed]
54. Inouye, M.; Chiba, J.; Nakazumi, H. Glucopyranoside Recognition by Polypyridine-Macrocyclic Receptors Pos-sessing a Wide Cavity with a Flexible Linkage. *J. Org. Chem.* **1999**, *64*, 8170–8176. [CrossRef] [PubMed]
55. Cheng, M.-J.; Tsai, I.-L.; Chen, I.-S. Chemical Constituents from Strychnos Cathayensis. *J. Chin. Chem. Soc.* **2001**, *48*, 235–239. [CrossRef]
56. Zhou, B.-D.; Weng, Z.-M.; Tong, Y.-G.; Ma, Z.-T.; Wei, R.-R.; Li, J.-L.; Yu, Z.-H.; Xu, G.-F.; Fang, Y.-Y.; Ruan, Z.-P. Syntheses of Xanthone Derivatives and Their Bioactivity Investigation. *J. Asian Nat. Prod. Res.* **2021**, *23*, 271–283. [CrossRef]
57. Santos, C.M.M.; Freitas, M.; Fernandes, E. A Comprehensive Review on Xanthone Derivatives as α-Glucosidase Inhibitors. *Eur. J. Med. Chem.* **2018**, *157*, 1460–1479. [CrossRef]
58. Liu, Y.; Ma, L.; Chen, W.-H.; Park, H.; Ke, Z.; Wang, B. Binding Mechanism and Synergetic Effects of Xanthone De-rivatives as Noncompetitive α-Glucosidase Inhibitors: A Theoretical and Experimental Study. *J. Phys. Chem. B* **2013**, *117*, 13464–13471. [CrossRef]

59. Cheng, Y.; Prusoff, W.H. Relationship between the Inhibition Constant (K1) and the Concentration of Inhibitor Which Causes 50 per Cent Inhibition (I50) of an Enzymatic Reaction. *Biochem. Pharmacol.* **1973**, *22*, 3099–3108. [CrossRef]
60. Ramsay, R.R.; Tipton, K.F. Assessment of Enzyme Inhibition: A Review with Examples from the Development of Monoamine Oxidase and Cholinesterase Inhibitory Drugs. *Molecules* **2017**, *22*, 1192. [CrossRef]
61. Geronimo, I.; Denning, C.A.; Heidary, D.K.; Glazer, E.C.; Payne, C.M. Molecular Determinants of Substrate Affinity and Enzyme Activity of a Cytochrome P450BM3 Variant. *Biophys. J.* **2018**, *115*, 1251–1263. [CrossRef]
62. Trott, O.; Olson, A.J. AutoDock Vina: Improving the Speed and Accuracy of Docking with a New Scoring Function, Efficient Optimization, and Multithreading. *J. Comput. Chem.* **2010**, *31*, 455–461. [CrossRef]
63. Schrödinger Release 2022-1: Maestro, Schrödinger, LLC, New York, NY. 2021. Available online: https://www.schrodinger.com/ (accessed on 10 December 2021).
64. Sankar, V.; Maida Engels, S.E. Synthesis, Biological Evaluation, Molecular Docking and in Silico ADME Studies of Phenacyl Esters of N-Phthaloyl Amino Acids as Pancreatic Lipase Inhibitors. *Future J. Pharm. Sci.* **2018**, *4*, 276–283. [CrossRef]
65. Chahinian, H.; Bezzine, S.; Ferrato, F.; Ivanova, M.G.; Perez, B.; Lowe, M.E.; Carrière, F. The B5′ Loop of the Pancre-atic Lipase C2-like Domain Plays a Critical Role in the Lipase−Lipid Interactions. *Biochemistry* **2002**, *41*, 13725–13735. [CrossRef] [PubMed]
66. Almasri, I.M. Computational Approaches for the Discovery of Natural Pancreatic Lipase Inhibitors as Antiobesity Agents. *Future Med. Chem.* **2020**, *12*, 741–757. [CrossRef] [PubMed]